Helmholtz solitons in diffusive Kerr-type media

Julio Sánchez-Curto* and Pedro Chamorro-Posada
Departamento de Teoría de la Señal y Comunicaciones e Ingeniería Telemática, Universidad de Valladolid, ETSI Telecomunicación, Paseo Belén 15, 47011 Valladolid, Spain
(Received 1 November 2015; published xxxxxx)

Soliton evolution at diffusive Kerr-type media is analyzed within the framework of the Helmholtz theory. The angular limitations of previous paraxial studies are overcome when both soliton propagation and diffusion of carriers are allowed to occur along any arbitrary direction. A model including two-dimensional carrier diffusion is proposed and its exact soliton solutions within the weakly nonlocal regime are presented. The restriction of carrier diffusion to a single transverse coordinate leads to the breakdown of the rotational symmetry of the Helmholtz framework and soliton behavior becomes angular dependent. We study the impact of this limitation in an intrinsic angular scenario, such as a nonlinear interface.

DOI: 10.1103/PhysRevA.00.003800

I. INTRODUCTION

Nonlocal media hosting soliton propagation have enriched the already existing vast field of spatial solitons [1,2]. Thermal media [3] or photorefractive materials [4] have been shown to accommodate thermal [5] or photorefractive [6,7] solitons, respectively. More recently, the reorientational ability of the molecules of a liquid crystal in the nematic phase has been found to induce optical confinement, so that a new type of solitary wave or nematicon can arise [8–10]. Nonlocality hasbeen essential not only in the description of new soliton families, but also in its ability to ease the comprehension of soliton dynamics [11–13] or to overcome certain scenarios that the traditional local models have failed to describe [14–16]. In other cases, the nonlocal response has been essential in the description of higher-order solutions [17,18], soliton interactions [19], and boundary [20,21] and interface [22–24] effects. The works on nematicons at interfaces have been the basis for the design and implementation of nematic crystal valves, which have been proposed as candidates for optical switching devices [25–27].

Regardless of the nature of nonlocal phenomena, soliton propagation in nonlocal media is usually studied using the nonlinear Schrödinger (NLS) equation where the slowly varying envelope approximation (SVEA) is assumed. The scalar nature of the NLS equation has restricted the study of soliton propagation in nonlocal media to broad beams (in relation to its wavelength) that propagate at vanishingly small angles (in relation to the evolution axis). The first type of limitation is overcome when one performs a full vectorial analysis based on Maxwell equations [28,29] that accounts for the small soliton width in relation to its wavelength. This approach has been applied to the study of anisotropic dielectrics where the nonparaxial framework alone has revealed substantial changes in relation to their paraxial counterparts [30,31].

The second restriction involved in the NLS equation, however, is essentially an angular limitation which is removed provided the SVEA is not assumed in the two-dimensional (2D) scalar Helmholtz equation [32]. Described by a scalar model, this type of nonparaxiality deals with broad beams propagating at arbitrary angles and it has been developed in the framework of the Helmholtz theory [33,34], where, for local media, essential corrections to previous paraxial studies have been revealed [35–39]. As regards nonlocal media, longitudinal nonlocal effects have been considered in liquid crystals [40] and, more recently, in thermal media [41]. Even within paraxial propagation contexts, the rapid evolution of the refractive index along the propagation direction must be preserved to accurately describe scenarios where soliton breathing arises or when losses are considered [41]. This type of on-axis nonparaxiality is, however, not addressed in our work. We focus, instead, on the off-axis nonparaxiality arising when shape-preserving beams do not propagate strictly parallel to the longitudinal axis, so that a full angular treatment of the problem is desirable [9,42].

We rely again on the Helmholtz theory to study soliton propagation in a diffusive Kerr-type medium where the nonlocal response accounts for the diffusion of carriers that takes place when an optical filed propagates in certain Kerr-type media [43]. However, in order to obtain an adequate description of soliton evolution at arbitrary angles, a full 2D model for the diffusion of carriers preserving the rotational invariance of the Helmholtz framework is required. Otherwise, the results are shown to exhibit a dependence on the propagation angle.

This paper is structured as follows. Section II presents the 2D model that rules soliton evolution for diffusive Kerr-type media within the limits of the weakly nonlocal regime. In Sec. III, we study the effects of the breakdown of the rotational symmetry inherent to the Helmholtz framework introduced when carrier diffusion is restricted to a single direction. In Sec. IV, the exact soliton solution for the nonlocal Helmholtz model with 2D carrier diffusion is presented and analyzed. We finally consider, in Sec. V, an inherent angular scenario, such as a nonlinear interface. Section VI summarizes the main conclusions of this work.

II. THE MODEL

The time-independent complex field envelope $E(x,z)$ of a continuous-wave TE-polarized beam evolves according to a

*julsan@tel.uva.es

2D Helmholtz equation,

$$\frac{\partial^2 E}{\partial z^2} + \frac{\partial^2 E}{\partial x^2} + \frac{\omega^2}{c^2} n^2 E = 0, \tag{1}$$

where n is the refractive index. This can be decomposed into a linear and a nonlinear part as $n^2 = n_l^2 + 2n_l\delta n$, where δn is the field-induced refractive index [43] described by a diffusion equation

$$D^2 \nabla_{xz}^2 \delta n - \delta n + \alpha |E|^2 = 0, \tag{2}$$

where D and α are, respectively, the diffusion and Kerr coefficients.

If we consider a forward-propagating beam $E(x,z) = (2\kappa n_l/\alpha)^{1/2} u(x,z) e^{jkz}$ and employ the normalizations $\zeta = z/L_D$ and $\xi = 2^{1/2} x/w_0$, w_0 being a transverse scale parameter equal to the waist of a reference Gaussian beam of diffraction length $L_D = k w_0^2/2$, Eqs. (1) and (2) are transformed into

$$\kappa \frac{\partial^2 u}{\partial \zeta^2} + i \frac{\partial u}{\partial \zeta} + \frac{1}{2} \frac{\partial^2 u}{\partial \xi^2} + \phi u = 0 \tag{3}$$

and

$$d_0^2 \left(\frac{\partial^2 \phi}{\partial \xi^2} + 2\kappa \frac{\partial^2 \phi}{\partial \zeta^2} \right) - \phi + |u|^2 = 0, \tag{4}$$

respectively. In this set of transformations $\kappa = 1/k^2 w_0^2$ is a nonparaxiality parameter [32,33], d_0 is the normalized diffusion coefficient $d_0^2 = 2D^2/w_0^2$, and $\phi = \delta n/2\kappa n_l$ is the normalized field-induced refractive index. Equations (3) and (4) govern soliton evolution in diffusive Kerr-type media within the Helmholtz nonparaxial framework. Since no assumptions have been made in their derivation, they are fully equivalent to their corresponding Helmholtz and diffusion equations, shown in Eqs. (1) and (2), respectively.

According to Eq. (4) the diffusion process can thus take place along any arbitrary direction in the xz plane, since no angular limitation is assumed within the Helmholtz theory. This imposes an essential difference in relation to previous paraxial work [44], which, restricted to vanishingly small angles of propagation, considers only diffusion along the transverse coordinate,

$$d_0^2 \frac{\partial^2 \phi}{\partial \xi^2} - \phi + |u|^2 = 0. \tag{5}$$

Equation (4) represents a generalization of Eq. (5) which can be properly used only in those scenarios restricted to very small angles of propagation where $\partial^2\phi/\partial\zeta^2 \to 0$. The use of Eq. (5) has been, however, recently proposed to describe soliton evolution at the interface separating diffusive Kerr-type media [45]. We show in Sec. III that in this case the rotational invariance inherent to the Helmholtz framework is broken and the properties of soliton propagation at large angles may be affected.

A. Weakly nonlocal regime

The study of nonlocal media traditionally distinguishes between weakly and strongly nonlocal regimes, depending on the extent of the response function of the nonlocal media in relation to the optical beam width [44]. When the response function is small compared to the beam width, one works within a weakly nonlocal regime which is mathematically addressed in a paraxial context provided $d_0^2 \ll 1$ [44]. In our Helmholtz framework, however, the weakly nonlocal approximation deserves further analysis since the angular content of the problem is also involved.

Equation (4) can be rewritten in the Fourier domain as

$$\Phi(k_\xi, k_\zeta)\left(1 + d_0^2 k_\xi^2 + 2\kappa d_0^2 k_\zeta^2\right) = U(k_\xi, k_\zeta), \tag{6}$$

where k_ξ and k_ζ are the transverse and wave numbers, respectively, and $H(k_\xi, k_\zeta) = (1 + d_0^2 k_\xi^2 + 2\kappa d_0^2 k_\zeta^2)^{-1}$ is the 2D Fourier transform of the response function $R(\xi,\zeta)$. $U(k_\xi, k_\zeta)$ and $\Phi(k_\xi, k_\zeta)$ denote the 2D Fourier transforms of $|u(\xi,\zeta)|^2$ and $\phi(\xi,\zeta)$, respectively. The response function associated with $H(k_\xi, k_\zeta)$ is

$$\begin{aligned} R(\xi,\zeta) &= \frac{1}{4\pi^2} \int_{-\infty}^{+\infty} \int_{-\infty}^{+\infty} \frac{e^{j\xi k_\xi} e^{j\zeta k_\zeta} dk_\xi dk_\zeta}{1 + d_0^2 k_\xi^2 + 2\kappa d_0^2 k_\zeta^2} \\ &= \frac{1}{2\pi d_0^2 \sqrt{2\kappa}} K_0\left(\frac{1}{d_0} \sqrt{\xi^2 + \frac{\zeta^2}{2\kappa}} \right) \end{aligned} \tag{7}$$

for $(\xi,\zeta) \neq (0,0)$ [46]. K_0 denotes the modified Bessel function of the second kind and zero order and its decaying rate is ruled by d_0^{-1}, so that in the local limit ($d_0 \to 0$) one has $R(\xi,\zeta) \to \delta(\xi,\zeta)$. When the response function is narrow in relation to the field intensity, the normalized field-induced refractive index $\phi(\xi,\zeta) = R(\xi,\zeta) * |u(\xi,\zeta)|^2$ can be calculated based on its 2D Taylor expansion. Since Eq. (7) verifies that [47]

$$\int_{-\infty}^{+\infty} \int_{-\infty}^{+\infty} R(\xi,\zeta) d\xi d\zeta = 1 \tag{8}$$

and

$$\frac{1}{2} \int_{-\infty}^{+\infty} \int_{-\infty}^{+\infty} \xi^2 R(\xi,\zeta) d\xi d\zeta = d_0^2, \tag{9}$$

one obtains

$$\phi(\xi,\zeta) \approx |u|^2 + d_0^2 \frac{\partial^2 |u|^2}{\partial \xi^2} + 2\kappa d_0^2 \frac{\partial^2 |u|^2}{\partial \zeta^2}. \tag{10}$$

Equation (10) provides an explicit expression for the normalized field-induced refractive index in the weakly nonlocal regime, which is the sum of the local Kerr contribution plus a nonlocal term that accounts for the diffusion processes along both transverse and longitudinal coordinates.

The substitution of Eq. (10) into Eq. (3) leads to

$$\begin{aligned} \kappa \frac{\partial^2 u}{\partial \zeta^2} + i \frac{\partial u}{\partial \zeta} + \frac{1}{2} \frac{\partial^2 u}{\partial \xi^2} + u\left(|u|^2 + d_0^2 \frac{\partial^2 |u|^2}{\partial \xi^2} + 2d_0^2 \kappa \frac{\partial^2 |u|^2}{\partial \zeta^2} \right) \\ = 0, \end{aligned} \tag{11}$$

which governs the propagation of solitons at wide angles in diffusive Kerr-type media with a weakly nonlocal response. Equation (11) represents a generalization of the equation found under the paraxial approximation [44], where the term $\kappa \partial^2/\partial\zeta^2 \to 0$ is neglected.

B. Angular restrictions

Equation (10) also reveals that the Fourier transform of the response function under the weakly nonlocal approximation

is $H(k_\xi,k_\zeta) \approx 1 - d_0^2 k_\xi^2 - 2\kappa d_0^2 k_\zeta^2$, which allows us to obtain the set of conditions that address the weakly nonlocal regime within the Helmholtz framework $d_0 k_\xi \ll 1$ and $\sqrt{2\kappa} d_0 k_\zeta \ll 1$. The maximum longitudinal and transverse wave numbers corresponding to the maximum angle of propagation $\theta = 90^o$ are, respectively, $k_{\zeta,\max} = 1/2\kappa$ and $k_{\xi,\max} = 1/(2\kappa)^{1/2}$ [33]. In this case, the former conditions are transformed into one, $d_0 \ll (2\kappa)^{1/2}$, which establishes the range of parameters where the weakly nonlocal approximation is valid for all angles of propagation. However, this is a very strict condition which can hardly be fulfilled in our scalar Helmholtz framework where $\kappa \ll 1$. In unscaled coordinates, one has $D \ll \lambda/(2\pi)$ revealing that the extent of the diffusion process should be even much less than the optical wavelength.

Since we work with broad beams, the validity of this approximation will be restricted to those angles whose transverse wave number verifies $k_\xi \ll d_0^{-1}$. The strength of the diffusion process thus limits the angular range where the weakly nonlocal approximation is valid. This limitation is taken into account throughout this work, so that soliton parameters are chosen to verify at least $k_\xi < d_0^{-1}$.

III. ONE-DIMENSIONAL DIFFUSION MODEL

Exact soliton solutions of the NLS equation with 1D carrier diffusion have been presented in [44]. The assumption that carrier diffusion takes place only along the transverse coordinate is adequate within the paraxial propagation regime. This model has been generalized to a Helmholtz equation including the same type of restricted transverse diffusion [45], which reads

$$\kappa \frac{\partial^2 u}{\partial \zeta^2} + i \frac{\partial u}{\partial \zeta} + \frac{1}{2} \frac{\partial^2 u}{\partial \xi^2} + u|u|^2 + d_0^2 \frac{\partial^2 |u|^2}{\partial \xi^2} u = 0. \quad (12)$$

Compared to Eq. (11), Eq. (12) retains the rapid evolution of the field envelope along the ζ coordinate but, simultaneously, discards the contribution of the diffusion process along the same coordinate.

The general exact soliton solution of Eq. (12) is

$$\pm(\xi + Vz) = 2d_0 \tan^{-1}(2d_0\sigma') + \frac{\sqrt{1+2\kappa V^2}}{\eta_0} \tanh^{-1}\left(\frac{\sigma'\sqrt{1+2\kappa V^2}}{\eta_0}\right), \quad (13)$$

where η_0 is the soliton peak amplitude, V represents the soliton transverse velocity, and σ' is the normalized soliton intensity [44],

$$\sigma'^2 = \frac{\eta_0^2 - \eta^2}{1 + 2\kappa V^2 + 4d_0^2\eta^2}. \quad (14)$$

The phase has an explicit expression,

$$\varphi(\xi,\zeta) = -V\xi \frac{\sqrt{1+2\kappa\eta_0^2}}{\sqrt{1+2\kappa V^2}} + \frac{\zeta}{2\kappa}\left(-1 \pm \frac{\sqrt{1+2\kappa\eta_0^2}}{\sqrt{1+2\kappa V^2}}\right). \quad (15)$$

Figure 1 plots the soliton transverse profiles given by Eqs. (13) and (14) for a diffusive Kerr-type medium with $d_0 = 0.14$ and a local Kerr medium ($d_0 = 0.0$) when two different transverse velocities are employed. As shown for $V = 8.4$, where the solid and dotted lines are almost superimposed, the angular correction can even mask the nonlocal contribution.

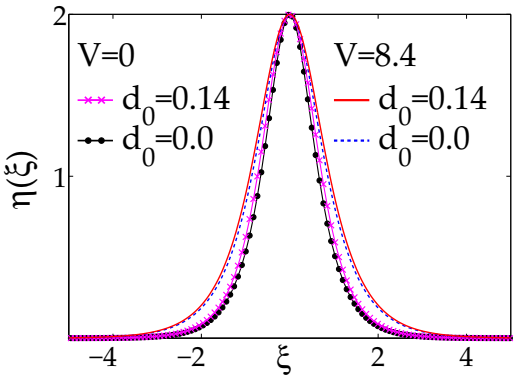

FIG. 1. Soliton transverse profiles for different diffusion coefficients and transverse velocities with 1D carrier diffusion. In all cases, $\eta_0 = 2$ and $\kappa = 5e-3$.

This effect can be mathematically captured taking into account the relationship between the transverse velocity and the actual angles of propagation θ $\tan\theta = (2\kappa)^{1/2} V$ [33], so that Eq. (14) can be rewritten as

$$\sigma' = \cos\theta \sqrt{\frac{\eta_0^2 - \eta^2}{1 + 4d_0^2\cos^2\theta\eta^2}} = \frac{D_\theta}{d_0}\sqrt{\frac{\eta_0^2 - \eta^2}{1 + 4D_\theta^2\eta^2}}. \quad (16)$$

In Eq. (16) we have defined an angular diffusion coefficient,

$$D_\theta = d_0 \cos\theta, \quad (17)$$

revealing that the impact of the nonlocal response on soliton evolution depends on the angle of propagation. As the angle of propagation increases nonlocal effects vanish. This can be seen when Eq. (13) is evaluated in the limit $\theta \to 90^o$ or, equivalently, $D_\theta \to 0$. While the first term in Eq. (13) becomes negligible,

$$\lim_{D_\theta \to 0} 2d_0 \tan^{-1}\left(2D_\theta\sqrt{\frac{\eta_0^2 - \eta^2}{1 + 4D_\theta^2\eta^2}}\right) = 0, \quad (18)$$

the hyperbolic function

$$\lim_{D_\theta \to 0} \tanh^{-1}\left(\frac{1}{\eta_0}\sqrt{\frac{\eta_0^2 - \eta^2}{1 + 4D_\theta^2\eta^2}}\right) = \tanh^{-1}\left(\frac{\sqrt{\eta_0^2 - \eta^2}}{\eta_0}\right) \quad (19)$$

remains independent of d_0, so that one recovers the solution for local Kerr media [33]. As the propagation angle increases and the beam direction departs from the ζ axis, the transverse nonlocal effects become negligible and local effects prevail. Therefore, soliton behavior becomes angle dependent when carrier diffusion along the ζ axis is neglected.

IV. NONLOCAL HELMHOLTZ SOLITONS

We now introduce the exact soliton solutions of the rotationally symmetric Helmholtz equation, (11), including 2D

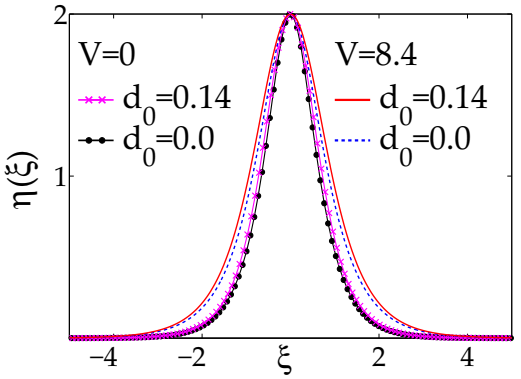

FIG. 2. Soliton transverse profiles for different diffusion coefficients and transverse velocities with 2D carrier diffusion. In all cases, $\eta_0 = 2$ and $\kappa = 5e-3$.

carrier diffusion effects and analyze their properties. Using the ansatz $u(\xi,\zeta) = \eta(\xi,\zeta)\exp(i\varphi(\xi,\zeta))$ with the sole assumption that φ is a linear combination of both ξ and ζ, the amplitude of the nonlocal Helmholtz soliton $\eta(\xi,\zeta)$ can be expressed in implicit form as

$$\frac{\pm(\xi + Vz)}{\sqrt{1+2\kappa V^2}} = 2d_0 \tan^{-1}(2d_0\sigma) + \eta_0^{-1}\tanh^{-1}\left(\sigma\eta_0^{-1}\right), \tag{20}$$

where

$$\sigma^2 = \frac{\eta_0^2 - \eta^2}{1+4d_0^2\eta^2}, \tag{21}$$

plus a phase term identical to that of Eq. (15).

The nonlocal Helmholtz soliton solution preserves the rotational symmetry inherent to the Helmholtz framework. One can easily check that Eqs. (20) and (21) can also be obtained after rotating in the Helmholtz framework the corresponding on-axis solution, $u(\xi,\zeta) = v(\xi)\exp(i\varphi(\zeta))$ [48]. In contrast to Eq. (13), Eq. (20) shows that the nonlocal Helmholtz soliton width preserves its dependency on the nonlocal contribution even when large angles of propagation are involved. This is shown in Fig. 2, where soliton transverse profiles for $V = 8.4$ are no longer superimposed when compared with their corresponding counterparts in Fig. 1.

The behavior of the nonlocal Helmholtz soliton is numerically tested by computing the numerical integration of Eq. (11) using the nonparaxial beam propagation method [49]. The contour plots in Fig. 3 display soliton evolution in diffusive Kerr-type media with $d_0 = 0.2$ (left) and $d_0 = 0.1$ (right) at two transverse velocities.

The power flow of the nonlocal Helmholtz soliton is

$$P_f = \int_{-\infty}^{+\infty}\left(\frac{1}{2\kappa} + \frac{\partial\varphi(\xi,\zeta)}{\partial\xi}\right)|u(\xi,\zeta)|^2 d\xi = \sqrt{1+2\kappa\eta_0^2}\left[\eta_0 + \frac{1+4d_0^2\eta_0^2}{2d_0}\tan^{-1}(2d_0\eta_0)\right] \tag{22}$$

and remains independent of the angle of propagation. Simulations have been designed to test the validity of Eq. (22). The numerical computation of the integral shown in Eq. (22)

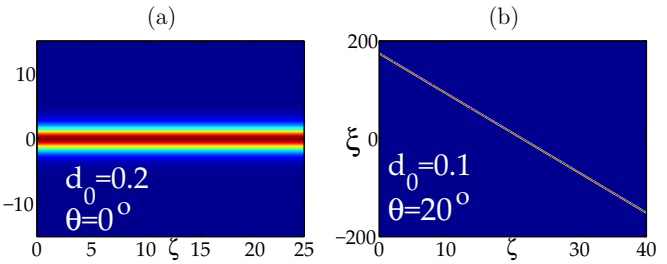

FIG. 3. Nonlocal Helmholtz solitons propagating in diffusive Kerr-type media (a) on axis and (b) off axis, $\theta = 20^\circ$. In all cases, $\eta_0 = 1$ and $\kappa = 1e-3$.

is plotted with symbols in Fig. 4, while horizontal lines correspond to the analytical result. The agreement between theory and numerics is excellent for all values tested.

This result differs from the one obtained for power flow of the solution given by Eqs. (13)–(15) when the 1D model for carrier diffusion is assumed. In this case, the power flow

$$P_f = \sqrt{1+2\kappa\eta_0^2}\left[\eta_0 + \frac{1+4D_\theta^2\eta_0^2}{2D_\theta}\tan^{-1}(2D_\theta\eta_0)\right] \tag{23}$$

depends on the angle of propagation through D_θ, so that the breakdown of the rotational symmetry manifests again. This is illustrated in Fig. 5(a), where Eq. (23) is displayed as a function of the angle of propagation for different values of d_0 and η_0.

While dotted horizontal lines account for Eq. (22), solid black lines represent the power flow in local Kerr media for $\eta_0 = 1$ and $\eta_0 = 2$ [48]. These two limits constitute, respectively, the maximum and minimum values that Eq. (23) may exhibit. Only for very small angles of propagation $\theta \to 0$ do the power flows of the 1D and 2D diffusion models agree. As $\theta \to 90^\circ$ and local effects prevail, the power flow tends to the one obtained for local Kerr media. The result of numerical simulations shown in Fig. 5(b) reinforces the angular dependence of the power flow when the 1D model is assumed and reveals the good agreement between theory (lines) and numerics (circles, diamonds, and squares).

We now test the validity of the weakly nonlocal regime approximation used so far compared to the complete nonlocal model represented by Eqs. (3) and (4). The field-induced

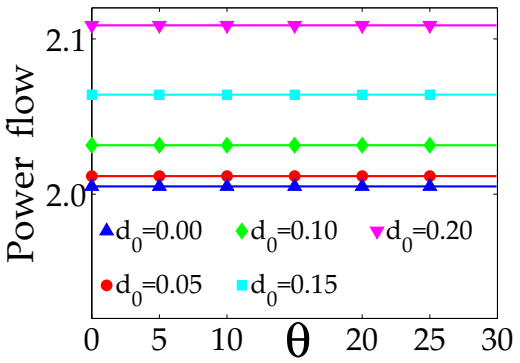

FIG. 4. Soliton power flow for different diffusion coefficients and transverse velocities. In all cases, $\eta_0 = 1$ and $\kappa = 2.5e-3$.

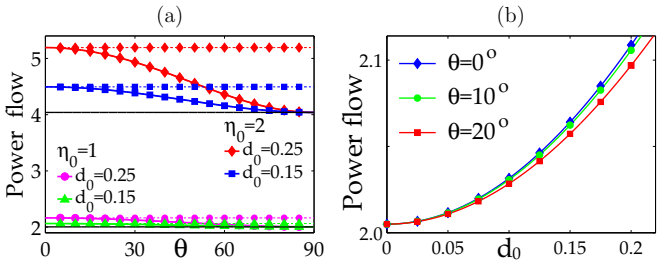

FIG. 5. (a) Power flow dependence on the angle of propagation for different amplitudes and diffusion coefficients with 1D carrier diffusion. (b) Numerical results for the power flow with 1D carrier diffusion. In all cases, $\kappa = 2.5e-3$.

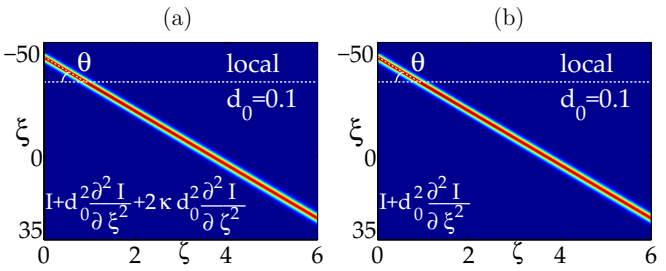

FIG. 6. Soliton evolution at an interface separating local and nonlocal media when (a) the 2D and (b) the 1D diffusion models are used.

refractive index given by Eq. (10) is substituted into Eq. (4) to obtain an estimation of the error assumed upon taking the approximation

$$\Delta\phi = \max\left\{\left|d_0^2\left(\frac{\partial^2\phi}{\partial\xi^2} + 2\kappa\frac{\partial^2\phi}{\partial\zeta^2}\right) + |u|^2 - \phi\right|\right\}. \quad (24)$$

Equation (24) can be rewritten as

$$\Delta\phi = d_0^4 \max\left\{\left|\frac{\partial^4|u|^2_{\theta=0}}{\partial\xi^4}\right|\right\}, \quad (25)$$

where $|u|^2_{\theta=0}$ denotes the intensity of the soliton propagating along the longitudinal axis.

V. NONLINEAR INTERFACES

In Secs. III and IV, we have shown that the study of diffusive Kerr-type media can be properly addressed only when the diffusion of carriers can occur along any arbitrary direction. Otherwise, the inherent rotational symmetry of the Helmholtz framework is broken and results have been demonstrated to exhibit an angular dependence. It is essential to take this into consideration when one works in nonlinear scenarios that have an inherent angular character, such as nonlinear interfaces [50–53]. Interfaces separating diffusive Kerr-type media have been traditionally studied within the paraxial framework, where modifications to the traditional local models have been reported [54,55]. More recently, the study of such interfaces has been performed in the Helmholtz framework assuming the 1D model described in Sec. III [45]. Nevertheless, this analysis is strictly valid only provided that vanishingly small angles of propagation are involved. The possible impact of this shortcoming is analyzed in the example below.

Figure 6 represents soliton evolution at the interface separating local and nonlocal diffusive Kerr-type media with $d_0 = 0.1$. Solitons, initially propagating in a local medium, impinge a nonlinear interface at an angle of incidence θ, thus undergoing refraction. Soliton evolution in the second medium has been computed twice, depending on the carrier diffusion model assumed. While the 2D model relies on the numerical integration of Eq. (11), the 1D model is based on Eq. (12).

The two pictures in Fig. 6 are visually very similar, although differences can be appreciated under a careful evaluation of the soliton parameters such as the peak amplitude and width. Figure 7 represents the evolution of the soliton peak amplitude for three angles of incidence when the 2D (dotted lines with filled symbols) and 1D (solid lines with open symbols) models are used. Since a sech-type beam is not the exact solution for diffusive Kerr-type media, the beam undergoes breathing upon entering the second medium. For small angles of incidence, such as 10° or less, differences between the two models are negligible. Dotted and solid lines with circles are almost superimposed. However, as the angle of incidence increases, the evolution of the soliton peak amplitude displays noticeable differences. The 2D model exhibits a lower peak amplitude, which corresponds to a larger soliton width. The diffusion process is enhanced since carriers can diffuse not only along the transverse, but also along the longitudinal coordinate.

Differences between the two models become more explicit at interfaces where, in addition to different diffusion coefficients, local mismatchings, $\Delta = (n_{l,1}^2 - n_{l,2}^2)/n_{l,1}^2$ and $\alpha = \alpha_2/\alpha_1$, come into play. Such an interface is shown in the two pictures of Fig. 8, which illustrate the evolution of a soliton that initially travels in a nonlocal medium ($d_{01} = 0.2$) and impinges the interface at an angle $\theta = 10.44°$.

The only difference between the two pictures in Fig. 8 is due to the model assumed for soliton propagation in the first medium, which is 2D in Fig. 8(a) and 1D in Fig. 8(b). The whole field-induced refractive index in the first medium is slightly raised in the 2D case, which makes the critical angle increase. That explains why the soliton propagating at an angle

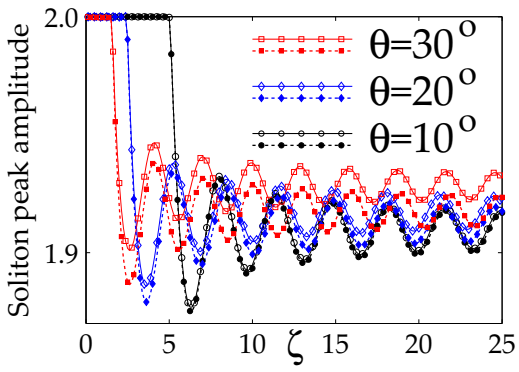

FIG. 7. Evolution of the soliton peak amplitude for an interface between a local and a diffusive Kerr-type medium with $d_0 = 0.1$. In all cases, $\eta_0 = 2$ and $\kappa = 1e-3$.

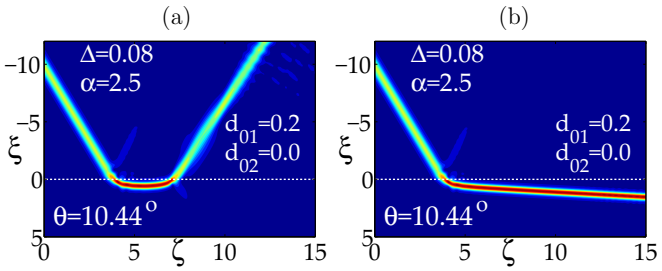

FIG. 8. Soliton evolving at the same interface when (a) a 2D and (b) a 1D propagation model is assumed in the first medium.

close to the critical angle undergoes internal reflection in the former case but refraction in the latter.

Optical switching devices based on soliton reflection and refraction have been proposed for diffusive Kerr-type media [56], photorefractive materials [57,58], and nematic liquid crystals [23,24], where the paraxial approximation has been assumed. Our nonparaxial approach can overcome this limitation and aid the understanding of experiments based on soliton reflection and refraction when nonvanishingly small angles are involved. The study of this type of nonlocal interfaces is the basis for a forthcoming work on this topic.

VI. CONCLUSIONS

In this work we have studied the propagation of solitons in diffusive Kerr-type media within the framework of the Helmholtz theory. Our analysis is valid for wide angles of propagation as long as a 2D model for the diffusion of carriers is considered. Exact soliton solutions have been presented and their power flow analysed. A model that only accounts for carrier diffusion along the transverse coordinate breaks the rotational symmetry of the Helmholtz framework, thus restricting its validity to angles of propagation that are not too large. This limitation has been analyzed with an example involving nonlinear interfaces. The validity of our findings has been computationally contrasted with the numerical integration of the corresponding evolution equations, showing an excellent agreement between theory and numerics.

ACKNOWLEDGMENTS

This work was supported by the Spanish Ministerio de Economía y Competitividad, Project No. TEC2015-69665-R.

[1] S. Trillo and W. Torruellas, *Spatial Solitons* (Springer-Verlag, Berlin, 2000).
[2] Z. Chen, M. Segev, and N. Christodoulides, Rep. Prog. Phys. **75**, 086401 (2012).
[3] M. D. Iturbe-Castillo, J. J. Sánchez-Mondragón, and S. Stepanov, Opt. Lett. **21**, 1622 (1996).
[4] G. C. Duree, Jr., J. L. Shultz, G. J. Salamo, M. Segev, A. Yariv, B. Crosignani, P. Di Porto, E. J. Sharp, and R. R. Neurgaonkar, Phys. Rev. Lett. **71**, 533 (1993).
[5] F. Derrien, J. Henninot, M. Warenghem, and G. Abbate, J. Opt. A: Pure Appl. Opt. **2**, 332 (2000).
[6] M. Segev, B. Crosignani, A. Yariv, and B. Fischer, Phys. Rev. Lett. **68**, 923 (1992).
[7] D.N. Christodoulides and M. I. Carvalho, J. Opt. Soc. Am. B **12**, 1628 (1995).
[8] G. Assanto, M. Peccianti, and C. Conti, Opt. Photon. News **14**, 44 (2003).
[9] M. Peccianti, C. Conti, G. Assanto, A. De Luca, and C. Umeton, Nature **432**, 733 (2004).
[10] M. Peccianti and G. Assanto, Phys. Rep. **516**, 147 (2012).
[11] A. W. Snyder and D. J. Mitchell, Science **276**, 1538 (1997).
[12] D. J. Mitchell and A. W. Snyder, J. Opt. Soc. Am. B **16**, 236 (1999).
[13] C. Conti, M. Peccianti, and G. Assanto, Phys. Rev. Lett. **91**, 073901 (2003).
[14] D. Suter and T. Blasberg, Phys. Rev. A **48**, 4583 (1993).
[15] O. Bang, W. Krolikowski, J. Wyller, and J. J. Rasmussen, Phys. Rev. E **66**, 046619 (2002).
[16] W. Krolikowski, O. Bang, N. I. Nikolov, D. Neshev, J. Wyller, and J. J. Rasmussen, J. Opt. B **6**, S288 (2004).
[17] D. Buccoliero, A. S. Desyatnikov, W. Krolikowski, and Y. S. Kivshar, Phys. Rev. Lett. **98**, 053901 (2007).
[18] D. Deng and Q. Guo, J. Opt. A: Pure Appl. Opt. **10**, 035101 (2008).
[19] M. Peccianti, K. Brzadkiewicz, and G. Assanto, Opt. Lett. **27**, 1460 (2002).
[20] B. Alfassi, C. Rotschild, O. Manela, M. Segev, and D. N. Christodoulides, Opt. Lett. **32**, 154 (2007).
[21] F. Ye, Y. V. Kartasov, B. Hu, and L. Torner, Opt. Lett. **34**, 2658 (2009).
[22] F. Ye, Y. V. Kartashov, and L. Torner, Phys. Rev. A **77**, 033829 (2008).
[23] M. Peccianti, A. Dyadyusha, M. Kaczmarek, and G. Assanto, Nat. Phys. **2**, 737 (2006).
[24] M. Peccianti, G. Assanto, A. Dyadyusha, and M. Kaczmarek, Phys. Rev. Lett. **98**, 113902 (2007).
[25] A. Piccardi, U. Bortolozzo, S. Residori, and G. Assanto, Opt. Lett. **34**, 737 (2009).
[26] A. Alberucci, A. Piccardi, U. Bortolozzo, S. Residori, and G. Assanto, Opt. Lett. **35**, 390 (2010).
[27] A. Piccardi, A. Alberucci, U. Bortolozzo, S. Residori, and G. Assanto, IEEE Photon. Technol. Lett. **22**, 694 (2010).
[28] S. Chi and Q. Guo, Opt. Lett. **20**, 1598 (1995).
[29] A. Ciattoni, B. Crosignani, P. Porto, and A. Yariv, J. Opt. Soc. Am. B **22**, 1384 (2005).
[30] A. Alberucci and G. Assanto, Opt. Lett. **36**, 193 (2011).
[31] A. Alberucci and G. Assanto, Phys. Rev. A **83**, 033822 (2011).
[32] G. Fibich, Phys. Rev. Lett. **76**, 4356 (1996).
[33] P. Chamorro-Posada, G. S. McDonald, and G. New, J. Mod. Opt. **45**, 1111 (1998).
[34] P. Chamorro-Posada, G. S. McDonald, and G. New, J. Opt. Soc. Am. B **19**, 1216 (2002).
[35] P. Chamorro-Posada and G. S. McDonald, Phys. Rev. E **74**, 036609 (2006).

[36] J. M. Christian, G. S. McDonald, and P. Chamorro-Posada, Phys. Rev. E **74**, 066612 (2006).
[37] J. M. Christian, G. S. McDonald, and P. Chamorro-Posada, Phys. Rev. A **76**, 033833 (2007).
[38] J. Sánchez-Curto, P. Chamorro-Posada, and G. S. McDonald, Opt. Lett. **32**, 1126 (2007).
[39] J. Sánchez-Curto, P. Chamorro-Posada, and G. S. McDonald, Phys. Rev. A **83**, 013828 (2011).
[40] D. W. McLaughlin, D. J. Muraki, M. J. Shelley, and X. Wang, Physica D **88**, 55 (1995).
[41] A. Alberucci, C. P. Jisha, N. F. Smyth, and G. Assanto, Phys. Rev. A **91**, 013841 (2015).
[42] C. Conti, M. Peccianti, and G. Assanto, Phys. Rev. E **72**, 066614 (2005).
[43] E. M. Wright, W. J. Firth, and I. Galbraith, J. Opt. Soc. Am. B **2**, 383 (1985).
[44] W. Krolikowski and O. Bang, Phys. Rev. E **63**, 016610 (2000).
[45] Z. Shi, Q. Guo, and H. Li, Phys. Rev. A **88**, 063848 (2013).
[46] M. Abramowitz and I. A. Stegun, *Handbook of Mathematical Functions* (Dover, Mineola, NY, 1972).
[47] I. S. Gradshteyn and I. M. Ryzhik, *Table of Integrals, Series, and Products* (Academic Press, San Diego, CA, 2007).
[48] P. Chamorro-Posada, G. S. McDonald, and G. New, J. Mod. Opt. **47**, 1877 (2000).
[49] P. Chamorro-Posada, G. S. McDonald, and G. New, Opt. Commun. **192**, 1 (2001).
[50] D. Mihalache, M. Bertolotti, and C. Sibilia, Prog. Opt. **27**, 229 (1989).
[51] A. B. Aceves, J. V. Moloney, and A. C. Newell, Phys. Rev. A **39**, 1809 (1989).
[52] A. D. Boardman, P. Egan, F. Lederer, and D. Mihalache, in *Nonlinear Surface Electromagnetic Phenomena*, edited by H. E. Ponath and G. I. Stegeman (North-Holland, Amsterdam, 1991), pp. 73–287.
[53] N. N. Akhmediev, in *Nonlinear Surface Electromagnetic Phenomena*, edited by H. E. Ponath and G. I. Stegeman (North-Holland, Amsterdam, 1991), pp. 289–321.
[54] P. Varatharajah, A. B. Aceves, J. V. Moloney, and E. M. Wright, J. Opt. Soc. Am. B **7**, 220 (1990).
[55] P. Varatharajah, A. C. Newell, J. V. Moloney, and A. B. Aceves, Phys. Rev. A **42**, 1767 (1990).
[56] R. Cuykendall and K. Strobl, J. Opt. Soc. Am. B **6**, 877 (1989).
[57] A. D. Boardman, P. Bontemps, W. Ilecki, and A. A. Zharov, J. Mod. Opt. **47**, 1941 (2000).
[58] E. Alvarado-Méndez, R. Rojas-Laguna, J. G. Aviña-Cervantes, M. Torres-Cisneros, J. A. Andrade-Lucio, J. C. Pedraza-Ortega, E. A. Kuzin, J. J. Sánchez-Mondragón, and V. Vysloukh, Opt. Commun. **193**, 267 (2001).